Growth shape of ^{3}He needle crystals

Etienne Rolley, Sébastien Balibar, and François Graner
Laboratoire de Physique Statistique, Ecole Normale Supérieure, 24, rue Lhomond, 75231 Paris Cedex, 05 France
(Received 7 October 1993)

We present experiments on the growth shape of ^{3}He needle crystals. These crystals show a surprisingly weak sidebranching. Growth velocities v and the tip radii ρ have been measured, and $v\rho^2$ is found to be roughly constant. We also measured the surface tension anisotropy. We compare our results with the microscopic solvability theory, which needs to be modified due to the existence of a thermal (Kapitza) resistance R_K at the interface. By studying the linear stability of a spherical seed, we show that R_K can be taken into account by modifying the ratio of the bulk heat conductivities. The selected values v and ρ at the tip are found, in satisfactory agreement with the modified theory. Some qualitative arguments are also presented which may explain the weakness of the sidebranching instability.

PACS number(s): 68.70.+w, 61.50.Cj, 67.80.−s, 68.45.−v

I. INTRODUCTION

It is now well known that dendrites grown from undercooled melt have their trip radius ρ and tip velocity v uniquely determined by the undercooling Δ [1–6]. Moreover, it was found that the product $v\rho^2$ is roughly constant [1,2,4–6]. The mechanism which determines the operating point is now better understood, but theoretical predictions have not yet received strong experimental confirmation.

The first step in the theory of dendritic growth is to look for steady-state solutions (needle crystal), and to study their linear stability. The characteristics of this needle crystal are assumed to be identical to those of the real dendrite, which, however, exhibits sidebranching at a distance from the tip which is usually a few ρ. Most recent theoretical works are based on the *microscopic solvability* approach [7], and predict that the value of the "stability parameter" $\sigma = 2d_0 D/v\rho^2$ is selected by the anisotropy ε in the surface tension. Here d_0 is a capillary length, and D the diffusivity. Up to now, most calculations were done in a two- (2D) or three-dimensional (3D) axisymmetric geometry. Recent attempts [8] have been made to deal with the full three-dimension dendrite, and the results do not seem very different from the 2D case. Comparison with experiment requires a precise measurement of the surface-tension anisotropy ε, which is difficult to obtain. According to Muscol, Liu, and Cummins [9], who performed careful measurements of ε in the case of succinonitrile and pivalic acid, the agreement between theory and experiment is not satisfactory. The agreement seems better in the case of ammonium bromide [2] and hectaoctyloxytriphenylene [6], but experimental uncertainties make difficult a precise test of the existing theory.

In a second step, the occurrence of sidebranching has been studied in the context of the linear stability of the needle crystal. One usually considers the sidebranching as resulting from the combined effects of the selective amplification of noise at the tip, and the advection of the perturbations away from the tip [10]. Though this assumption seems qualitatively confirmed by experiments [11], the detailed time-dependent behavior of sidebranches is not yet completely understood.

In this context, ^{3}He appears as a very unusual and interesting system. Indeed, at $T \approx 0.1$ K, we observed that ^{3}He crystals grow usually as almost perfect needles. Such an observation has almost never been reported [12]. We tried to find out if this peculiar behavior of ^{3}He could be explained at least in the frame of the existing theory.

We have measured v and ρ, and computed the value of the stability parameter σ. We have independently estimated ε. Direct comparison with theoretical prediction is not possible in the case of ^{3}He because the standard assumption of thermodynamic equilibrium at the interface is no longer valid. The Kapitza resistance R_K of the solid-liquid interface is not negligible, which modifies the usual form of the Gibbs-Thomson relation. We have taken R_K into account using a spherical approximation for the tip of the crystal. This crude approximation gives a good agreement between experimental and theoretical values of σ.

Thus the selection of the operating point seems to have received a satisfactory answer from standard theory. This is not the case for the weakness of the sidebranching, and we only present an attempt to explain the needle shape of ^{3}He crystals.

The paper is organized as follows. In Sec. II, we describe the experimental apparatus and techniques, and we present our results. In Sec. III, we write down the modified equations for crystal growth, which take into account the Kapitza resistance, and solve them for a spherical geometry. Section IV contains the discussion of the results.

II. EXPERIMENT

A. Experimental setup and crystal growth

The experimental setup was built to study the roughening transition in ^{3}He. It has been described in detail in

previous papers [13]. We recall only the main features of the apparatus. ^{3}He crystals are grown in a cylindrical cell of 4-mm diameter and 5-mm length, which is closed by two sapphire windows. The cell is completely immersed in superfluid ^{4}He, and sintered copper allows good thermalization between the ^{4}He bath and the cell. The upper part of the cell is a double Be-Cu membrane, whose inner volume depends on the pressure of the surrounding bath: a 5% change in the cell volume can be obtained. Changing the ^{4}He pressure allows us to grow or melt the crystal at constant mass. The temperature is measured with a Speer carbon resistor placed in the ^{4}He bath. We used the melting curve of ^{3}He for the calibration of the thermometer.

Because of the strong minimum in the melting pressure of ^{3}He (at 0.32 K), we usually obtain growing crystals in the following way. We first fill the cell with liquid at high temperature (near 0.5 K), just below the melting pressure. Then we decrease the temperature: the crystal first grows, but begins to melt as soon as the temperature is lower than 0.32 K. It disappears at a temperature of order 0.1 K. At this temperature, the filling capillary is blocked with solid. We regulate the temperature and slowly increase the pressure by acting on the Be-Cu membrane. We thus obtain growing crystals at constant temperature. It should be noted that most of our experiments were performed at temperatures such that the latent heat is negative. The ^{3}He we used for this experiment contained 200 ppm of ^{4}He.

Crystals usually nucleate on several points of the cell. Below 0.32 K, they nucleate on hot spots such as dirt on the windows (Fig. 1). We tried to control the nucleation site by applying a high voltage (of order 500 V) to a needle, in order to create a strong local electric field. This technique had been successful in ^{4}He but did not work in ^{3}He. This is probably due to some residual thermal gradient whose effect is bigger than that of the electric field.

To avoid the influence of the finite geometry, the walls and neighboring crystals have to be far enough from the one under study. More quantitatively, the typical distance between the crystal and the walls should be larger than the diffusion length $l=D/v$, where D is the diffusivity [14]. We only used those runs where one or two isolated crystals grew, as illustrated in Fig. 1. Such events happen, but are quite rare, and this is the main reason why our data are not very numerous.

During the first few minutes, the growth is usually observed to be quasistationary, both ρ and v being constant. When the crystal length reaches a few millimeters, the velocity decreases, due to a decreasing of the undercooling. In the following, we selected data corresponding to sequences where the speed of the tip is constant over at least 2 mm.

B. Experimental results

The successive profiles were recorded either with a video camera or, more often, by taking photographs, which were later digitalized with a plotter and a microcomputer (Fig. 2). The interface is defined as the darkest line of the profile. The speed v is calculated from the positions of the tip; we obtain values ranging from 3 to 50 μm/s, at various temperatures from 80 to 120 mK. The tip radius of curvature is obtained by a least-squares parabolic fit of the profile (Fig. 3), and is of order 10 μm. The determination of ρ is easy and precise, as the profile is an almost perfect parabola. The Peclet number $\rho v/2D$ lies in the range 10^{-3}–10^{-2}, which means that ρ is small with respect to the diffusion length D/v. This is the domain of validity of most theoretical calculations.

The main experimental results are the following.

(i) Though there is a large scatter in our results, we found that $v\rho^2$ is roughly constant, as expected. There is no clear dependence on $v\rho^2$ either with v or with temperature (Fig. 4). The mean value is

$$v\rho^2=(7.6\pm1.5)\times10^3\ \mu\text{m}^3/\text{s}\ .$$

In these calculations, we assumed that the tip is moving perpendicularly to the observation axis because the field depth is small. However, this assumption has no reason to be strictly true, and the resulting uncertainty on v is about 10%. This could explain the dispersion in the data, and that is the reason why we did not make any more elaborate image analysis.

(ii) In most cases, crystals have needle shapes which are almost perfect parabolae. No systematic deviation can be

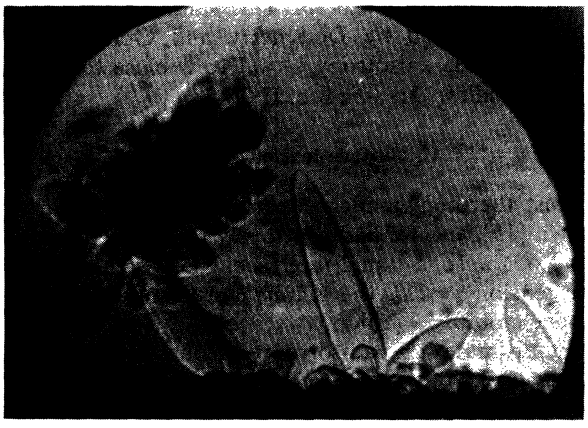

FIG. 1. Growing crystals at $T=97$ mK. The speed of the one in the center is 16 μm/s. The width of the cell is 4 mm.

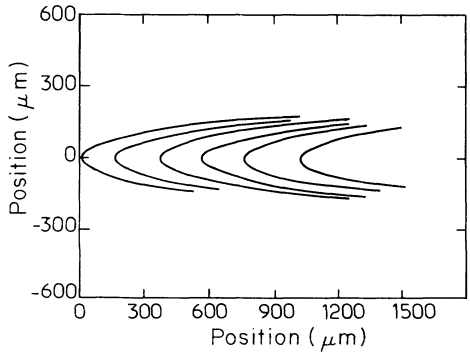

FIG. 2. Profiles of the needle crystal of Fig. 1 at successive times 0, 16, 27, 39, 52, and 68 s.

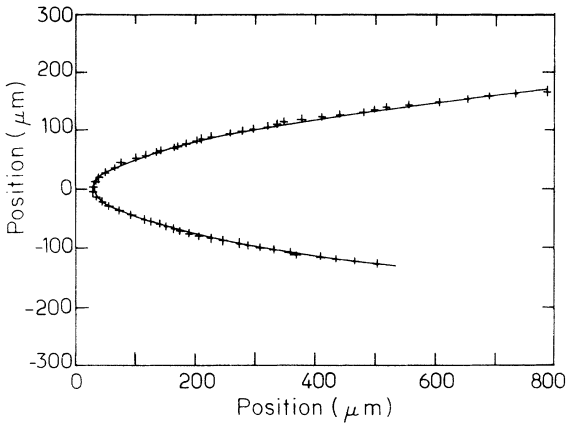

FIG. 3. Experimental profile (crosses) and best parabolic fit (solid line) of the crystal of Fig. 1.

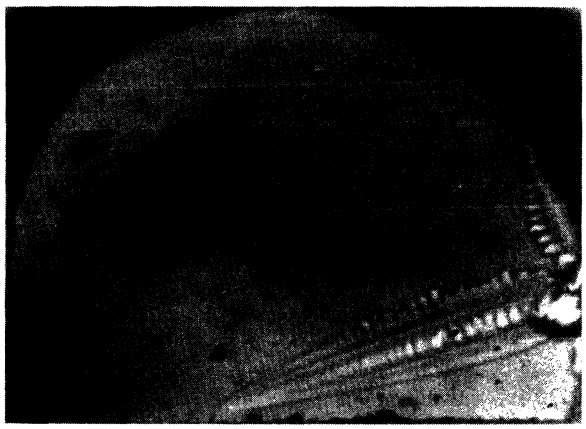

FIG. 5. Dendrite with sidebranching ($T=100$ mK, $v=30$ μm/s). The width of the cell is 4 mm.

seen between the experimental profile and the parabolic fit up to a distance 40ρ from the tip. To our knowledge, such shapes have only been observed in pure ^{4}He by Franck and Jung [12]. In their experiment, however, the diffusion length is of the same order as or larger than the size of the experimental cell, so that their crystals are far from being free dendrites. Moreover, the thermal diffusivities as well as the surface tension are not well known in their temperature range, thus making difficult a comparison with other systems.

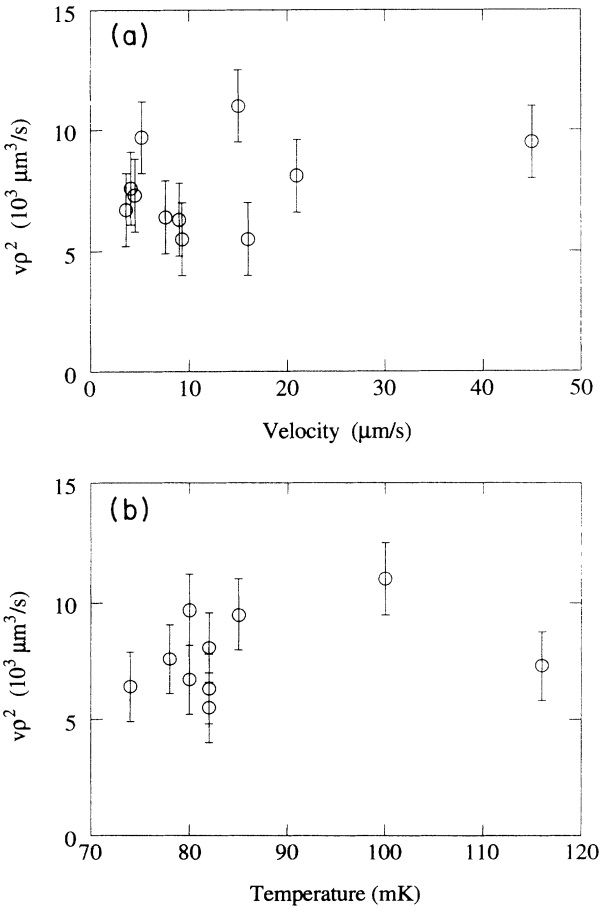

FIG. 4. Dependence of $v\rho^2$ on (a) speed and (b) temperature.

We do not think that ^{3}He crystals are stable with respect to sidebranching, but rather that this instability is very weak. Indeed, in the case of Fig. 5, where the dendrite is well isolated and the tip radius ρ small, side branches appear at a distance 50ρ from the tip. The needle shape we usually observed is due simply to the fact that we cannot look at the profile far enough from the tip. 50ρ is a surprisingly high value: in all other known systems [1–6,11], sidebranching starts much closer to the tip, and deviations from the parabolic shape are clear at 10ρ. Nevertheless, for the slowest dendrites, the diffusion length is comparable to the cell size. This could decrease the sidebranching instability; indeed, it can be seen in Fig. 5 that sidebranches are not visible on the stem close to the wall. Except for this particular run, we expect finite-size effects to be small, since we analyzed only data where the diffusion length l is equal or larger than the cell size l_0. Furthermore, the appearance of sidebranches does not depend on the ratio l/l_0.

In the only case where we could measure it (the crystal of Fig. 5), we found that the spacing between the sidearms λ was equal to 5ρ. This value is comparable to the one obtained by Dougherty and Gollub [2] with NH_4Br, whose anisotropy $\varepsilon=0.016$ is close to the value we obtained for ^{3}He (see Sec. II C).

C. Surface-tension anisotropy

Most thermodynamic properties of bulk ^{3}He are well known [15], and we had previously measured some properties of the solid-liquid interface, such as the mean surface tension γ [13], the Kapitza resistance R_K, and the surface mobility k [16].

To estimate the anisotropy of the surface tension, which turns out to be a key parameter in dendritic growth, we used the same method as Huang and Gliksmann [1] for succinonitrile and pivalic acid. We looked at the shape of small liquid inclusions in the solid (Fig. 6). The diameter of these droplets (0.3 mm) is small

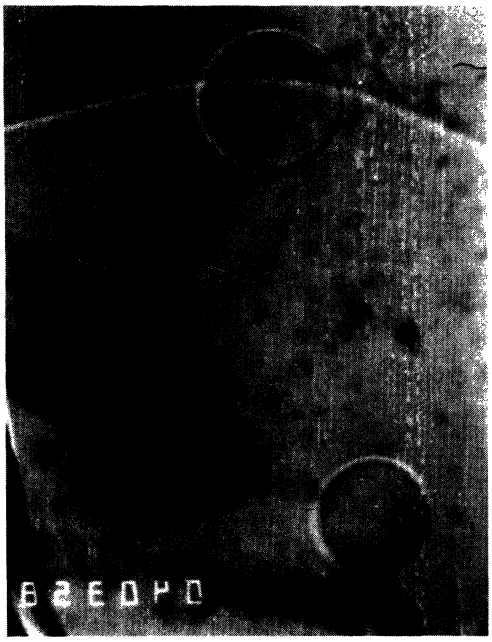

FIG. 6. Small quasispherical liquid inclusions (mean diameter 0.3 and 0.4 mm).

compared to the gravitational capillary length $\lambda=1.1$ mm [13]. The influence of gravity is thus negligible, and the anisotropy of a droplet is the same as that of the surface tension. Provided that the observation axis is along a (100) axis of the crystal, we can write the equation of the profile as $R=R_0(1+\varepsilon\cos4\theta)$. To first order in ε, the intersection of the surface tension polar plot with a (100) plane can then be written as $\gamma=\gamma_0(1+\varepsilon\cos4\theta)$ [9].

Unfortunately, we do not know the crystalline orientation of the droplets. So we perform a cosine Fourier analysis of the profile, writing the profile as $R=R_0[1+\sum_n a_n\cos(n\theta)]$. We choose the droplet where the fourfold symmetry is the strongest, and found for this droplet that the relative radius variation of the droplets is $\Delta r/r\approx0.02$, so that we estimated the anisotropy of the surface tension to be

$$\varepsilon\approx0.02\pm0.01 .$$

This value is of the same order of magnitude as other cubic crystals [4].

III. THEORETICAL BACKGROUND

A. Heat or impurity diffusion

The ^{3}He used in our experiment is rather pure: the only impurity is ^{4}He, whose concentration is 200 ppm, and heat diffusion is very likely to be the limiting process. We will indeed show that the impurities have a negligible effect.

The phase diagram of ^{3}He–^{4}He mixtures has been calculated by Edwards and Balibar [17]. From their results, we could determine the important parameter in our problem, namely the ratio K of the liquidus to the solidus slopes. The phase diagram is represented in Fig. 7, for a

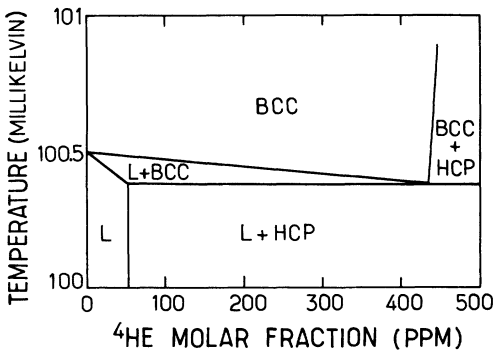

FIG. 7. Phase diagram of ^{3}He-^{4}He mixtures at pressure $P=30.90$ bar.

pressure $P=30.90$ bar which corresponds to a melting temperature of 0.1 K for pure ^{3}He. One notices that ^{4}He is 8.3 times more soluble in the solid than in the liquid phase at this temperature. As a consequence, when the crystal grows, impurities are absorbed instead of being rejected as usual. However, the mechanism of the Mullins-Sekerka instability is not changed by this peculiarity nor by the negative value of the latent heat.

It can also be seen that the maximum solubility in the liquid phase is 50 ppm near 0.10 K, though the initial concentration is 200 ppm. The excess ^{4}He could remain in the warmer upper part of the filling capillary because the maximum solubility increases strongly with temperature (the value is 200 ppm at 0.12 K). Or the system could be on the three-phase coexistence line: a hexagonal crystal of volume 10^{-3} mm^3 can contain the total amount of ^{4}He, and such a crystal could lie in some nonvisible part of the cell.

Let us suppose that the ^{4}He concentration is roughly 50 ppm. Recent models [18] have determined the influence of the coupling between heat and impurity diffusion. The product $v\rho^2$ depends on the impurity concentration C according to the following formula:

$$\frac{(v\rho^2)_{C=0}}{(v\rho^2)_C}=1+2\frac{mC(1-K)}{L/C_L}\frac{D_{\rm th}}{D_{\rm is}} ,$$

where $m=2.23\times10^{-3}$ mK/ppm is the slope of the liquidus, $K=8.3$, $C_L=0.719$ J/gK is the heat capacity of the liquid [19], and $D_{\rm th}$ and $D_{\rm is}$, respectively, are the thermal and isotopic diffusivity in the liquid phase. $D_{\rm th}=5.46\times10^{-4}$ cm^2/s [20]. $D_{\rm is}$ has been measured only at 0.5 K [21]. According to Edwards, Pettersen, and Culman [22], the value at 0.1 K should be about 15×10^{-4} cm^2/s. With $C=50$ ppm, we find that the change in $v\rho^2$ due to the amount of ^{4}He is less than 0.1%: the effect of impurities is small because the diffusion constants have the same order of magnitude, and the ^{4}He concentration is small. From now on, we thus neglect the effect of impurities.

B. The growth equations

Heat diffusion equations in bulk phases are the same in ^{3}He as in usual systems. The total heat balance at the in-

terface is not changed either. We thus write [23]

$$D_L \Delta T_L + \frac{\partial T_L}{\partial t} = 0 , \quad (1)$$

$$D_S \Delta T_S + \frac{\partial T_S}{\partial t} = 0 , \quad (2)$$

$$\rho_S L v = [-K_L(\nabla T_L) + K_S(\nabla T_S)] \cdot \mathbf{n} , \quad (3)$$

where T is the temperature, $D_{S,L}$ the thermal diffusivities, $K_{S,L}$ the heat conductivities, and $\rho_{S,L}$ the densities. The subscripts S or L stand for the solid or liquid phases. L is the latent heat per unit mass, and v the interface velocity. $\mathbf{n}$ is the unit normal at the interface, directed into the liquid. In the following, all extensive quantities will be expressed per unit mass.

In the case of ^{3}He, we have to modify the usual form of the Gibbs-Thomson relation, which requires thermodynamic equilibrium at the interface. Following Castaing and Nozières [24], the total heat current through the interface is $J_E = Q_S + TS_S J = Q_L + TS_L J$, where $J = \rho_S v$ is the mass current through the interface, $Q_{S,L}$ are the conductive heat flows in each phase and $S_{S,L}$ are the entropies of each phase. J_E and J are related to the differences of temperature and chemical potential across the interface by

$$T_L - T_S = R_K (J_E - \lambda J) ,$$

$$J = \rho_S k \left[(\mu_L - \mu_S) + \lambda \frac{T_L - T_S}{T} \right] .$$

The coefficient λ determines which fraction of each entropy is liberated or absorbed on each side of the interface. According to Balibar, Edwards, and Saam [25] and Graner, Bowley, and Nozières [26], all latent heat is liberated in the liquid, which means that the cross coefficient λ is equal to TS_S. This gives us

$$\mu_L - \mu_S = \frac{v}{k} - S_S (T_L - T_S) .$$

On the other hand, usual thermodynamics yield

$$\mu_L - \mu_S = -\frac{\gamma}{\rho_s}\kappa - \frac{L}{T^*}(T_L - T^*) - S_S (T_L - T_S)$$

where κ is the interface curvature, and T^* the melting temperature for a flat interface. We finally obtain

$$\frac{L}{T^*}(T_L - T^*) = -\frac{\gamma}{\rho_S}\kappa - \frac{v}{k} . \quad (4)$$

This is the usual Gibbs-Thomson relation, with an additional kinetic term. The fact that the $T_L - T_S$ term vanishes is the consequence of the very peculiar value of λ. Nevertheless, we have one more equation, which gives $T_L - T_S$:

$$T_L - T_S = R_K K_S \mathbf{n} \cdot \nabla T_S . \quad (5)$$

Here also, $T_L - T_S$ explicitly depends only on ∇T_S because $\lambda = TS_S$.

We are not able to solve this set of equations, i.e., to find stationary growth shapes, even if we neglect the kinetic term, which is a valid approximation in our case as shown below. In order to understand the effect of the Kapitza resistance, we perform a linear stability analysis for a growing sphere.

C. The growing sphere

It is easier to use the dimensionless variables $u_{L,S} = C_{L,S}(T_{L,S} - T^*)/L$. In the quasistationnary approximation, Eqs. (1)–(5) become:

$$\Delta u_L = 0 , \quad (1')$$

$$\Delta u_S = 0 , \quad (2')$$

$$v = -D_L(\nabla u_L - \eta \nabla u_S)\cdot \mathbf{n} \quad \text{where } \eta = \frac{K_S}{K_L} , \quad (3')$$

$$u_{L,\text{interface}} = -d_0 \kappa - k' v , \quad (4')$$

$$u_L - u_S = R_K K_S \mathbf{n} \cdot \nabla u_S . \quad (5')$$

In equation (4'), $d_0 = \gamma T^* C_L / L^2 \rho_s$ is a capillary length and $k' = T^* C_L / L^2 k$ is a growth resistance. From the mean value $\gamma = 0.06$ erg/cm^2 [13], and from the data of Graner, Balibar, and Rolley [16], we find $d_0 = 38$ Å and $k' = 4.3 \times 10^{-2}$ s/m. From the work of Greywall [20], we estimate the ration η to be about 220. All these values have been calculated for $T = 0.1$ K. The thermal conductivity of the solid is unusually larger than that of the liquid.

Let us first show that the growth resistance is negligible: for a typical dendrite $\rho = 20$ μm and $v = 20$ μm/s. We then find $d_0 \kappa \sim 10^{-4}$ and $k' v \sim 10^{-6}$. We thus recover the usual relation:

$$u_{L,\text{interface}} = -d_0 \kappa .$$

All the crystals considered here grow at velocities which are large enough for the dynamic roughening to occur [27], so that in order to calculate k' we have used measurements of k performed on a rough interface. Such an assumption is no longer valid as soon as the interface is close to the faceting. Indeed, we have estimated that $k'_{\text{facet}} / k'_{\text{rough}} \sim 10^3$, for a faceted crystal growing at 0.1 K, with $v = 1$ μm/s [13]. The velocity is thus a strongly nonlinear function of the undercooling: at the end of the growth, when the crystal begins to feel the influence of the wall, the speed decreases very abruptly as the interface becomes faceted. In the following calculation, we neglect the growth resistance as well as the anisotropy of the surface tension.

We can then perform the usual linear stability analysis [23] in an axisymmetric geometry. To first order, we write the crystal profile as $R = R_0[1 + \sum_j \rho_j Y_j(\theta)]$, where the functions $Y_j(\theta)$ are the spherical harmonics. Without the Kapitza resistance R_K, the threshold defined by $d\rho_j / dt = 0$ would be given by

$$\frac{R_0}{R_C} = 1 + \frac{(j-1)(j+2)(j+1+\eta j)}{2(j-2)} ,$$

where R_C is the critical nucleation radius. In order to take R_K into account, we find that η has to be replaced

by η_{eff}:

$$\eta_{\text{eff}}=\frac{\eta}{1+jR_K K_S/R_0} . \quad (6)$$

Taking the typical value of the tip radius (20 μm) for R_0, and $j=4$, the effective ratio of the heat conductivities η_{eff} is of order 0.5 instead of $\eta=200$. It means that the combined effect of the Kapitza resistance and the cross coefficient λ makes heat transport in the solid much less efficient. The physical explanation is the following [16,26]: during growth, latent heat is released on the liquid side of the interface. It can diffuse either in the liquid (the thermal resistance is then proportional to $1/K_L$) or the solid. In this case heat has first to cross the interface before diffusing in the solid. The thermal resistance involves two contributions being respectively proportional to $1/K_S$ and R_K.

A new length scale $R_K K_S \approx 3000$ μm appears in the stability problem. If the typical size R_0 of the crystal is much smaller than $R_K K_S$, the effect of the Kapitza resistance is dominant, and this favors the diffusion process in the liquid as $\eta_{\text{eff}} \ll \eta$. This is our case, as far as the tip of the dendrite is concerned.

On the other hand, if $R_0 \gg R_K K_S$, the Kapitza resistance is negligible, and the ratio of the heat conductivities recovers its usual value: $\eta_{\text{eff}} \approx \eta$.

IV. DISCUSSION

We have seen that the limiting diffusion process in our experiment is heat diffusion, and have calculated the capillary length d_0. From the measured value of $v\rho^2$, we can thus infer the value of the stability parameter σ:

$$\sigma_{\text{expt}}=\frac{2d_0 D}{v\rho^2}=0.058\pm0.011 .$$

Up to now, no theoretical work has been devoted to the problem of a free dendrite which includes irreversible thermodynamics at the interface. In order to discuss the value of σ_{expt} we make the following two assumptions.

(i) For a growing crystal of typical size ρ, ^{3}He is equivalent to a classical system, provided that the ratio η of the heat conductivities is replaced by $\eta_{\text{eff}}(\rho)$. For values of ρ ranging from 15 to 50 μm, η_{eff} lies between 0.2 and 1.

(ii) The standard model can be used to predict σ. We use the tip radius of curvature as a length scale to compute η_{eff}.

We can then calculate σ. For the symmetrical model ($\eta=1$), and with Pe=0 and $\varepsilon=0.02$, a numerical calculation in a 3D axisymmetric model gives $\sigma^*=0.045$ [28]. According to Barbieri and Langer [29], $\sigma(\eta)=[2/(1+\eta)]\sigma^*$. For our experiment, one thus expect values of σ to be in the range 0.045–0.075. This is consistent with the mean value σ_{expt}.

This may seem too simple a way to deal with a very complex system. Actually, we do not claim that we have solved the problem raised by the new thermodynamic equations at the interface. More accurate measurements of ε and $v\rho^2$ are needed in order to discuss our assumptions. In particular, if our approach is valid, one expects σ to vary as a function of ρ according to

$$\frac{\sigma(\rho)}{\sigma^*}=\frac{2}{1+\eta/[1+4R_K K_S/\rho]} . \quad (7)$$

The corresponding variation of σ is plotted in Fig. 8: though the large scatter in our experimental data, they are not in contradiction with Eq. (7).

At this point, it is quite satisfactory that standard theory gives a reasonable value for the operating point in a nonclassical system such as ^{3}He.

The most puzzling question may be the weakness of the sidebranching instability. According to the most commonly accepted scenario, sidebranching instability results in selected amplification of noise [10]. This scenario has not yet received strong experimental confirmation [11]. In our case, we can estimate the mean thermodynamic fluctuations of the temperature: $\delta T \approx T(k_B/C_V)^{1/2} \approx 10^{-8}$ K. In order to calculate the undercooling Δ, we use the Ivanstov relation [23]: $\Delta=\text{Pe}e^{\text{Pe}}E_1(\text{Pe})$, where Pe is the Péclet number and E_1 the exponential integral. The typical undercooling in our experiment is 10^{-5} K. The relative fluctuations of the undercooling are then $\delta\Delta/\Delta \approx 10^{-3}$. This is the same order of magnitude as found by Dougherty, Kaplan, and Gollub [11] for NH_4Br, where sidebranches appear much closer to the tip.

What is the peculiarity of ^{3}He which could be responsible for such a weak sidebranching?

(i) The interface is close to faceting, and the growth resistance could be large enough to decrease the noise amplification. However, experiments have been performed on NH_4Br [30] near its roughening transition. They have shown that dendrites develop ordinary sidebranches as soon as the tip velocity is typically ten times larger than the limit velocity where facets become macroscopic. This is the domain we have studied, so it seems unlikely that the roughening transition has an important effect.

(ii) Development of sidebranching involves larger length scales than the tip radius of curvature (for in-

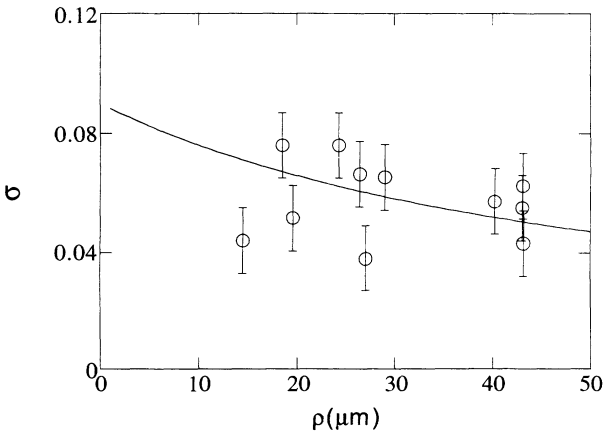

FIG. 8. Experimental data and expected theoretical variation of σ.

stance, the sidebranch spacing is of order 5ρ). From relation (7), one qualitatively expects the effective heat ratio to be much larger than 1. This means that heat diffusion through the solid phase becomes more important for such length scales, which in turn increases the stability of the interface. Though finite-size effects are presumably important in most of their experiments, it is interesting to come back to the results of Franck and Jung [12]. Crystals shown in Fig. 5 of Ref. [12] are very similar to our observations, i.e., sidebranching is very weak. Franck and Jung also estimate the ratio of the heat conductivities to be $\eta=7$. In usual materials, η is of order 1. Thus it seems to us that the unusual importance of heat transfer in the solid phase is a common feature of both experiments, and could be an explanation for the weakness of the sidebranching.

Though ^{3}He has some particular features which make the theoretical problem more complicated, further studies could bring about a better insight of dendritic growth. ^{3}He is a pure system whose thermodynamic properties are well known. Furthermore, many of them depend strongly on the temperature.

(i) d_0 diverges when T becomes close to 0.32 K (the latent heat vanishes),

(ii) R_K varies like T^{-3} [31]: η_{eff} is a strongly decreasing function of T.

Changing the temperature should thus make it possible to modify the important parameters in the problem.

ACKNOWLEDGMENT

The Laboratoire de Physique Statistique is "associé au CNRS et aux Universités Paris 6 et Paris 7."

[1] S. C. Huang and M. E. Gliksmann, Acta Metall. **29**, 701 (1981).
[2] A. Dougherty and J. P. Gollub, Phys. Rev. A **38**, 3043 (1988).
[3] J. H. Bilgram, M. Firman, and E. Hürlimann, J. Cryst. Growth **96**, 175 (1989).
[4] Ph. Bouissou, thèse de doctorat de l'Université Paris 6, 1989 (unpublished); M. E. Glicksman and N. B. Singh, J. Cryst. Growth **98**, 277 (1989).
[5] K. Koo, R. Ananth, and W. N. Gill, Phys. Rev. A **44**, 3782 (1991).
[6] P. Oswald, J. Phys. (France) **49**, 1083 (1988).
[7] J. S. Langer, Science **243**, 1150 (1989). For a review, see for example, D. A. Kessler and J. Koplik, Adv. Phys. **37**, 255 (1988).
[8] M. Ben Amar and E. Brener, Phys. Rev. Lett. (1993) (to be published).
[9] M. Muschol, D. Liu, and H. Z. Cummins, Phys. Rev. A **46**, 1038 (1992).
[10] J. S. Langer, Phys. Rev. A **36**, 3350 (1987).
[11] S. C. Huang and M. E. Gliksmann, Acta Metall. **29**, 717 (1981); A. Dougherty, P. D. Kaplan, and J. Gollub, Phys. Rev. Lett. **58**, 1652 (1987); X. W. Quian and H. Z. Cummins, *ibid.* **64**, 3038 (1990); E. Hürlimann, R. Trittibach, U. Bisang, and J. H. Bilgram, Phys. Rev. A **46**, 6579 (1992); P. Bouissou, A. Chiffaudel, B. Perrin, and P. Tabeling, Europhys. Lett. **13**, 89 (1990).
[12] J. P. Franck and J. Jung, J. Low Temp. Phys. **64**, 165 (1986).
[13] E. Rolley, S. Balibar, and F. Gallet, Europhys. Lett. **2**, 247 (1986).
[14] B. Janiaud, P. Bouissou, B. Perrin, and P. Tabeling, Phys. Rev. A **41**, 7059 (1990).
[15] E. R. Grilly, J. Low Temp. Phys. **4**, 615 (1971).
[16] F. Graner, S. Balibar, and E. Rolley, J. Low Temp. Phys. **75**, 69 (1989).
[17] D. O. Edwards and S. Balibar, Phys. Rev. B **39**, 4083 (1989).
[18] M. Ben Amar and P. Pelcé, Phys. Rev. A **39**, 4263 (1989).
[19] D. S. Greywall, Phys. Rev. B **27**, 2747 (1983).
[20] D. S. Greywall, Phys. Rev. B **29**, 4933 (1984).
[21] V. L. Vvedenskii and V. P. Peshkov, Pisma Zh. Eksp. Teor. Fiz. **23**, 643 (1976) [JETP Lett. **23**, 589 (1976)].
[22] D. O. Edwards, M. S. Pettersen, and T. G. Culman, J. Low Temp. Phys. **89**, 831 (1992).
[23] J. S. Langer, Rev. Mod. Phys. **52**, 1 (1980).
[24] B. Castaing and P. Nozières, J. Phys. (France) **41**, 701 (1980).
[25] S. Balibar, D. O. Edwards, and W. F. Saam, J. Low Temp. Phys. **82**, 119 (1991).
[26] F. Graner, R. M. Bowley, and P. Nozières, J. Low Temp. Phys. **80**, 113 (1990).
[27] P. Nozières and F. Gallet, J. Phys. (France) **48**, 353 (1987); F. Gallet, S. Balibar, and E. Rolley, *ibid.* **48**, 369 (1987); S. Balibar, F. Gallet, F. Graner, C. Guthmann, and E. Rolley, Physica B **169**, 209 (1991).
[28] M. Ben Amar (private communication).
[29] A. Barbieri and J. S. Langer, Phys. Rev. A **39**, 5314 (1989).
[30] J. Maurer, P. Bouissou, B. Perrin, and P. Tabeling, Europhys. Lett. **8**, 67 (1989).
[31] J. Amrit and J. Bossy, Europhys. Lett. **15**, 441 (1991).

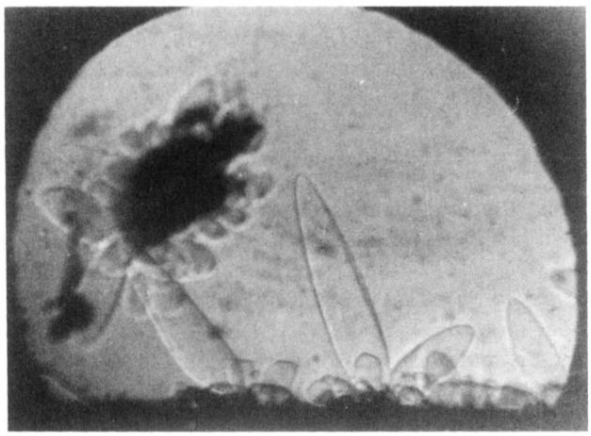

FIG. 1. Growing crystals at $T=97$ mK. The speed of the one in the center is 16 μm/s. The width of the cell is 4 mm.

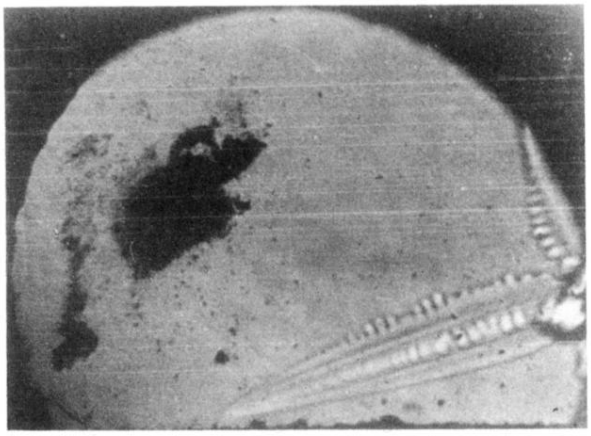

FIG. 5. Dendrite with sidebranching ($T=100$ mK, $v=30$ μm/s). The width of the cell is 4 mm.

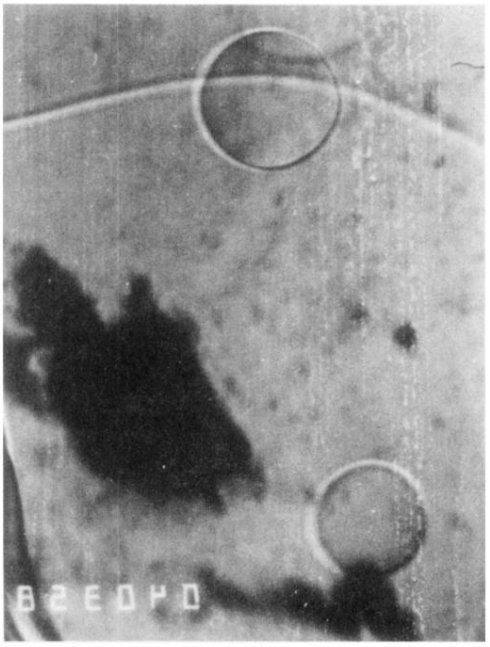

FIG. 6. Small quasispherical liquid inclusions (mean diameter 0.3 and 0.4 mm).